Fluid-flow characterization with nuclear spins without magnetic resonance

C. W. Crawford,[1,a)] Shoujun Xu,[1] Eric J. Siegel,[1] Dmitry Budker,[2] and Alexander Pines[1]
[1]*Materials Sciences Division, Lawrence Berkeley National Laboratory, Berkeley, California 94720, USA and Department of Chemistry, University of California, Berkeley, California 94720, USA*
[2]*Department of Physics, University of California, Berkeley, California 94720, USA and Nuclear Sciences Division, Lawrence Berkeley National Laboratory, Berkeley, California 94720, USA*

(Received 12 June 2008; accepted 10 August 2008; published online 5 September 2008)

A technique for noninvasive monitoring of flow inside metallic enclosures using laser-based atomic magnetometry is introduced. The analyte is labeled via nuclear magnetization by magnets, thereby combining the polarization and encoding steps. No radiofrequency or audiofrequency pulses are involved. We demonstrate detection of flow inside an aluminum pipe with an inner diameter of 4.9 mm that has a constriction with a diameter of 1.6 mm and a length of 6.4 mm. The results agree with a model of spin density and relaxation indicating that our technique allows for fast, quantitative, and noninvasive diagnostics of flow with potential applications discussed below. © *2008 American Institute of Physics*. [DOI: 10.1063/1.2977773]

Characterizing fluid flow is important in various medical and industrial applications, for instance, to diagnose pathologies[1–3] or to nondestructively characterize accumulation of sediment in pipes.[4,5] Industrial applications range from aeronautics to microfluidics.[6,7]

Various techniques have been used to study flow, including ultrasonic tomography,[8,9] optical coherence tomography (OCT),[3,10,11] and magnetic resonance imaging (MRI).[6,7] However, each of these techniques has its limitations. For example, OCT is largely limited to transparent samples, while conventional high-field MRI is incapable of imaging within metal enclosures or in the presence of magnetic-susceptibility gradients. MRI with alternative detection methods overcomes some of the problems, but encoding schemes are involved, which require pulses of resonant magnetic field and impose demanding requirements on the stability and homogeneity of the leading field in the interaction region.[12,13]

Here we show an approach for noninvasive monitoring of continuous flow that circumvents the limitations of high-field MRI; we use an atomic magnetometer to directly detect fluidic analytes labeled via enhanced nuclear magnetization through the exposure of the analyte to the magnetic field of permanent magnets. Only the nuclear spins exposed to this field are detected, in contrast to ultrasound or OCT where detection is unable to differentiate contributions to flow from different volumes. Because the magnetization is detected directly, no encoding pulses are needed.

The atomic magnetometer[14] based on nonlinear magneto-optical rotation with frequency-modulated light[15] was built in our laboratory. Two anti-relaxation-coated glass cells filled with rubidium-87 (Rb) are adjacent to the detection volume. Linearly polarized light tuned to the rubidium D1 line produces alignment of the ground state via optical pumping; the alignment precesses in the magnetic field at the Larmor frequency that is proportional to the average magnetic field across the cell and causes time dependent optical rotation. The polarization of the laser beams after they pass through the Rb vapor cells is monitored via balanced polarimeters. The two sensors form a gradiometer to cancel the applied bias field and eliminate common-mode noise.

Having been encoded by the permanent magnets, the water flows into a detection region. The polarized nuclear spins are subject in the detection region to a leading field of 0.5 G (B_l in Fig. 1) provided by a solenoid that pierces the magnetic shield. The introduction of the polarized water sample changes the magnetic field strength at the Rb cells and consequently the frequency of the magneto-optical resonance. The magnetometer therefore detects the magnetic field generated by the water sample.

Backed by high-pressure nitrogen (5.2 bar), water flows at 30 ml/min through a structured tube (Fig. 1, inset). The tube has four sections: section 0 is the outlet of the pipe that has negligible volume, sections 1 and 3 are not constricted (inner diameters of 4.9 mm) portions of the pipe, while section 2 is constricted (inner diameter of 1.6 mm). Sections 1–3 are 6.4 mm long. The water sample is magnetized by six $6.4\times6.4\times6.4$ mm^3 neodymium-iron-boron magnets ar-

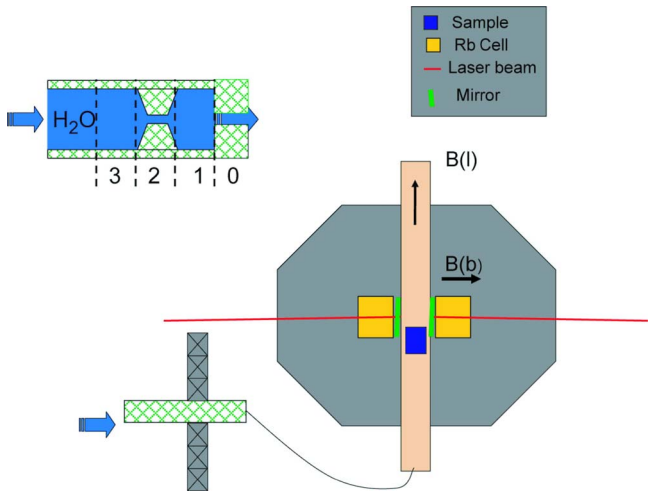

FIG. 1. (Color online) Schematic of flow characterization with an atomic magnetometer via nuclear magnetization labeling. The inset shows the structured pipe with a constricted area and the magnets (gray blocks) that are used for polarizing the water sample. The magnets are modulated perpendicular to the plane of the page and scanned in the plane of the page to characterize different sections.

a)Electronic mail: cwcraw@gmail.com.

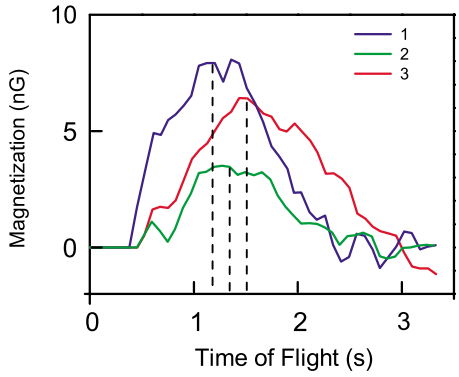

FIG. 2. (Color online) Flow averages (the magnetometer signal) when polarizing sections 1–3. These are the average of 50 modulation cycles where in each modulation cycle the magnets are brought into the vicinity of the tube at zero time for 1.5 s and are then removed for 1.5 s.

ranged with three on either side of a section. This creates a field of 3 kG between the magnets, which falls to 100 G at a distance, along the direction of flow, of 3 mm from the edge of the magnets. To distinguish the signal from slow drifts, the magnets are moved 2 cm away from the tube with a given frequency. (Note that electromagnets that would not require mechanical modulation can also be used.) To measure the internal structure of the tube, the magnets are placed along each section.

Temporal signal averages for sections 1–3 are obtained (Fig. 2). These are the signals from each modulation cycle averaged together; a modulation cycle of 1.5 s polarized and 1.5 s unpolarized is used. The characteristics of these signals are dictated by the distance of the encoding region from the detector and the volume of the encoding region. The peak from section 3 occurs ~0.3 s later than the peak from section 1, roughly corresponding to the time it takes to traverse that distance. The magnitude of the maximum signal of the former is consequently lower than that of the latter because of the relaxation and flow velocity dispersion that occur in the ~0.3 s. We see that section 2 shows the lowest signal of the three, a result of its small volume. A smaller volume increases the linear flow rate decreasing the residence time of the water in the constriction and consequently the magnetization.

To gain quantitative information, the raw modulation cycle signal from each section is Fourier transformed. For the data in Fig. 3, the magnets were modulated at 0.50 Hz, 1.0 s for polarization, corresponding to approximately 0.5 ml, and 1.0 s to separate the polarized-water volumes by unpolarized water. Measurements are performed for 50 modulation cycles at each position (100 s total time). The signal approximates a sine wave as the water in the encoding region gains magnetization but is not allowed to return to equilibrium because of the fast modulation frequency. The amplitude at 0.50 Hz represents the magnitude of signal from the modulation of the magnets. Figure 3(a) shows the Fourier transform of a measurement of section 1. A plot of the signal at 0.50 Hz as a function of the position of the magnet is shown in Fig. 3(b). The proton magnetization in the water depends on its residence time in the magnetic field and its travel time from the polarization region to the detection region. A simple model is constructed from this insight:

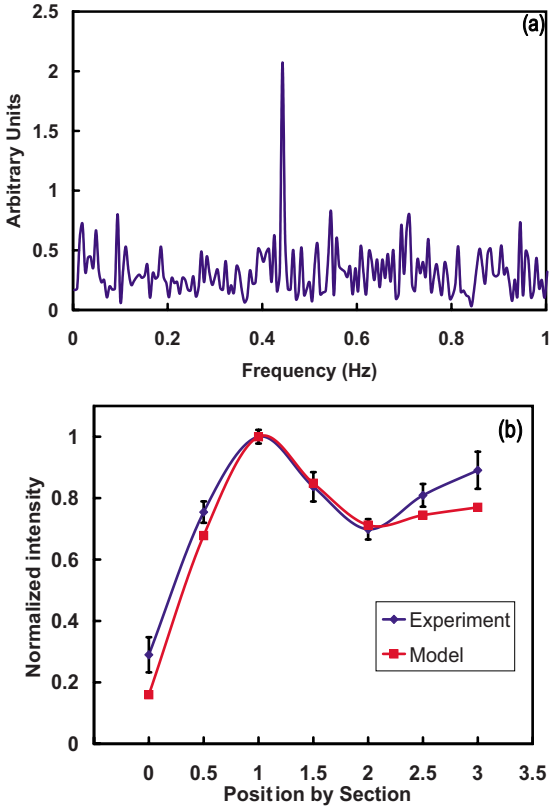

FIG. 3. (Color online) (a) Fourier transform of the raw data corresponding to a time series of 50 modulation cycles for section 1. The magnets are brought in and out for 1 s at a rate of 0.5 Hz. (b) Comparison of experimental signal (blue) with the model (red). Position is defined by which section is covered by the polarizing magnets. The value in section 1 is the measurement taken when the magnet completely covered section 1, while the value at section 1.5 is the value measured when the magnets covered half of section 1 and half of section 2.

$$M = M_0\left[1 - \exp\left(\frac{-v}{R_f T_1}\right)\right]\exp\left(\frac{-V}{R_f T_1}\right). \tag{1}$$

The first exponential term describes the magnetization that the sample gains during the encoding/polarization phase. The second exponential term accounts for the relaxation of the magnetization during the flow from the encoding region to the detection region. M_0 is the maximum magnetization that can be gained by thermal polarization from the magnetic field of the magnets, v is the volume of the section being magnetized, T_1 is the relaxation time of the nuclear magnetization (1.6 s for water with concentrations of oxygen[16] corresponding to equilibrium with the atmosphere), V is the total downstream between the encoding/polarization volume and the detector, and R_f is the volume flow rate. Overlaying the data in Fig. 3(b) are the results based on Eq. (1).

These signals can be used to calculate the volume of each section if the volume of one section is known,

$$\frac{S_1}{V_1} = \frac{S_2}{V_2}\exp\frac{V_1}{R_f T_1}. \tag{2}$$

Here S_1 and S_2 are the signals from sections 1 and 2, respectively, and V_1 and V_2 are the volumes for sections 1 and 2, respectively. Assuming that the volume in section 1 is known, the volume of section 2 is determined to be 0.090 cm^3, which is comparable to its measured volume of 0.096 cm^3. The model and experiment for section 3 show a

deviation of roughly 14%, as can be seen in Fig. 3. We see the rise in signal as expected but the signal is higher than predicted by the model. A more sophisticated model including factors such as flow dispersion would be required to account for the details of the observed signals. In our study we have used Eqs. (1) and (2) to calculate the volume of sections of the pipe; however, one could also imagine inverting the problem and calculating the flow rates from the known volumes.

The competition between polarization and relaxation allows a range of acceptable flow rates and measurement volumes. For a given flow rate a large-volume tube will lead to increased relaxation before it has reached the detector. A lower bound is dictated by the residence time in the encoding region. As volumes contract, the residence time decreases meaning less polarization is gained by the sample. Decreasing the flow rate will not only increase the polarization time but also the travel time. The characteristics of the system being examined would dictate the flow rate to balance these factors. If one moves the detection region to just after the encoding region, our model system can handle sections with a much larger volume. This would require a movable detection apparatus, allowing the detection region to be close to the changing encoding regions, which would be facilitated by miniature atomic magnetometers.[17,18] Consequently, systems that could be investigated include millimeter-to-centimeter-scale flow applications.

One possible application of the present technique is detecting blood flow at the intersection of blood vessels. A magnet could be appropriately positioned with respect to an artery or vein. A miniature magnetometer[17,18] could be placed on the patient, downstream from the polarization/encoding site. This arrangement would detect a volume separate from the encoding volume and would allow to characterize mixing in vessel junctions or spin relaxation occurring within the vessels. In combination with appropriate contrast agents, this may allow detection of abnormal tissues.

In conclusion, we note that instead of atomic magnetometers, other magnetic detectors can be used. However, anisotropic-magnetoresistance sensors and fluxgate magnetometers do not as yet possess sufficient sensitivity.[19,20] Superconducting quantum interference devices possess excellent sensitivity but require cryogenics and are typically not optimized for low-frequency operation.

We thank Dr. Andreas Trabesinger for stimulating discussion. We also thank David Michalak, Micah Ledbetter, and Victor Acosta for patiently reviewing this paper. This work was supported by the Director, Office of Science, Office of Basic Sciences, Materials Sciences Division of the U.S. Department of Energy (contract No. DE-AC02-05CH11231). D.B. acknowledges support by the Office of Naval Research Multidisciplinary University Research Initiative grant (contract No. FD-N00014-05-1-0406).

[1] S. Tanaka, T. Kitamura, M. Fujita, K. Nakanishi, and S. Okuda, AJR, Am. J. Roentgenol. **154**, 509 (1990).
[2] J. Schmitt, IEEE J. Quantum Electron. **5**, 1205 (1999).
[3] J. Izatt, M. Kulkarni, S. Yazdanfar, J. Barton, and A. Welch, Opt. Lett. **22**, 1439 (1997).
[4] V. Sukackas, Ultragarsas **49**, 16 (2003).
[5] V. Sukackas, Ultragarsas **2**, 23 (2005).
[6] S. Han, K. Pierce, and A. Pines, Phys. Rev. E **74**, 016302 (2006).
[7] C. Hilty, E. McDonnell, J. Granwehr, K. Pierce, S. Han, and A. Pines, Proc. Natl. Acad. Sci. U.S.A. **102**, 14960 (2005).
[8] C. Passmann and H. Ermert, IEEE Trans. Ultrason. Ferroelectr. Freq. Control **43**, 545 (1996).
[9] A. Vladisauskas, Ultragarsas **39**, 1 (2001).
[10] D. Huang, E. Swanson, C. Lin, S. Schuman, W. Stinson, W. Chang, M. Hee, T. Flotte, K. Gregory, C. Puliafito, and J. Fujimoto, Science **254**, 1178 (1991).
[11] W. Drexler, U. Morgner, R. Ghanta, F. Kartner, J. Schuman, and J. Fujimoto, Nat. Med. **7**, 502 (2001).
[12] R. McDermott, S. Lee, B. ten Haken, A. Trabesinger, A. Pines, and J. Clarke, Proc. Natl. Acad. Sci. U.S.A. **101**, 7857 (2006).
[13] S. Xu, V. Yashchuk, M. Donaldson, S. Rochester, and D. Budker, Proc. Natl. Acad. Sci. U.S.A. **103**, 12668 (2006).
[14] S. Xu, S. Rochester, V. Yashchuk, M. Donaldson, and D. Budker, Rev. Sci. Instrum. **77**, 083106 (2006).
[15] D. Budker, D. Kimball, V. Yashchuk, and M. Zolotorev, Phys. Rev. A **65**, 055403 (2002).
[16] K. Lee, M. Mößle, W. Myers, N. Kelso, A. Trabesinger, A. Pines, and J. Clarke, Magn. Reson. Med. **53**, 9 (2005).
[17] M. Balabas, D. Budker, J. Kitching, P. Schwindt, and J. Stalnaker, J. Opt. Soc. Am. B **23**, 6 (2006).
[18] V. Shah, S. Knappe, P. Schwindt, and J. Kitching, Nat. Photonics **1**, 649 (2007).
[19] S. Andreev and P. Dimitrova, J. Optoelectron. Adv. Mater. **7**, 199 (2005).
[20] A. Palacios, J. Aven, V. In, P. Longhini, A. Kho, J. Neff, and A. Bulsara, Phys. Lett. A **367**, 25 (2007).